



Electrochemical Activity of Electrodeposited V₂O₅ Coatings

D. Vernardou,^{a,b,c,z} A. Sapountzis,^c E. Spanakis,^{b,c} G. Kenanakis,^{a,b,d} E. Koudoumas,^{a,e} and N. Katsarakis^{a,b,d}

^aCenter of Materials Technology and Photonics, School of Applied Technology, Technological Educational Institute of Crete, 71004 Heraklion, Crete, Greece

^bScience Department, School of Applied Technology, Technological Educational Institute of Crete, 71004 Heraklion, Crete, Greece

^cDepartment of Materials Science and Technology, University of Crete, 71003 Heraklion, Crete, Greece

^dInstitute of Electronic Structure and Laser, Foundation for Research and Technology-Hellas, 71110 Heraklion, Crete, Greece

^eElectrical Engineering Department, Technological Educational Institute of Crete, 71004 Heraklion, Crete, Greece

Vanadium oxide microcrystallites are electrodeposited at room temperature. The effect of the deposition current density on the structural, morphological and electrochemical properties of the coatings is studied. The electrochemical activity of the material is found to improve with the deposition current density utilized during electrodeposition. At the highest deposition current values, marked amounts of lithium charge are observed to interchange with the material owing to the increased coverage of its structure. The highest specific capacitance of 145 F g⁻¹ measured in 1 M LiClO₄ is comparable to previously reported values using different electrolytes such as NaCl, LiCl and KCl.

© 2012 The Electrochemical Society. [DOI: 10.1149/2.054301jes] All rights reserved.

Manuscript submitted July 31, 2012; revised manuscript received September 19, 2012. Published November 6, 2012.

In recent decades, electrochemical capacitors (ECs) have attracted considerable attention because they promise longer lifetimes compared to rechargeable batteries and higher storage density compared to common capacitors.¹⁻³ These potentials make them good candidates for power sources in hybrid electric vehicles,⁴ camera-flash equipment, cellular phones and navigational devices.⁵ Charge-storage in ECs is mainly based on either a double-layer type capacitance or a charge-transfer-reaction pseudocapacitance. The double-layer capacitive process arises from the typical charge separation occurring between the electrode and an electrolyte,^{6,7} whereas the pseudocapacitive process arises from reversible faradaic redox reactions that occur at or near the active electrode surface.⁸ Compared with double-layer based capacitors, pseudocapacitors based on transition metal oxides could provide higher specific capacitance i.e. charge storage capability per utilized material mass but they suffer from disadvantages such as poor charging rates.⁹⁻¹²

Among the various transition metal oxides, vanadium pentoxide (V₂O₅) has been studied as the active material for electrochemical pseudocapacitor applications preliminary due to its low cost and its ability to exist in different oxidation states. Previous studies have demonstrated high charge storage density, complete reversibility upon discharging and stability over successive loading cycles.¹²⁻¹⁵ During the intercalation process, electrical energy is stored in the material bulk to be available for work upon release during the deintercalation process. Consequently, a large surface area, providing for ease of interaction with the electrolyte thus a fast charge transport, is one of the most important conditions necessary to achieve high intercalation/deintercalation rates¹⁶ contributing to enhanced EC's performance.

Many chemical routes, such as hydrothermal¹⁷ and sol-gel synthesis,¹⁸ chemical vapor¹⁹⁻²³ and electrochemical deposition²⁴⁻²⁹ have been used for the growth of vanadium oxides. Among those, electrodeposition has advantages such as simplicity and low cost of the setup and reaction materials, generally fast reaction rates at as low as room temperature and one disadvantage namely the need of a conductive substrate. Vanadium oxides have been electrodeposited mainly using VOSO₄ as the vanadium source at ≤65°C,^{24,25,27,29} while in some of these depositions, higher temperatures (350²⁶ and 200°C²⁸) were also utilized in the process.

Our approach, presented in this study, was to electrodeposit V₂O₅ using V₂O₅ in its powder form as the vanadium source, dissolved in methanol and water at room temperature. This is probably one of the simplest approaches, however never studied before in the literature,

to the best of our knowledge. The correlation of the morphology with the electrochemical activity, comprising charge storage capability and corresponding specific capacitance, dynamics, reversibility and repeatability of the charge transfer through the as-deposited vanadium oxides is investigated.

Experimental

The electrolyte for the deposition of vanadium oxide coatings was prepared by adding 0.9 g V₂O₅ powder in a solution of 60 mL CH₃OH (methanol) and 20 mL H₂O to form an orange suspension. Prior to electrodeposition, ITO (indium tin oxide) glass substrates were ultrasonically cleaned with 2-propanol, acetone, MilliQ H₂O and dried with N₂. Three series of experiments were performed using deposition current densities of a) 0.05 mA cm⁻², b) 0.10 mA cm⁻² and c) 0.25 mA cm⁻² for deposition periods of 10, 20 and 30 min in each case. Platinum, Ag/AgCl and ITO glass substrates were used as the counter, reference and working electrodes respectively. Finally, each freshly deposited sample was rinsed with water and dried in air at room temperature.

X-ray diffraction (XRD) measurements were performed using a Siemens D5000 Diffractometer for 2θ = 10.0–60.0 degs, step size 0.05 degs and step time 60 s/deg. Raman measurements were performed in a Nicolet Almega XR micro-Raman system using the 473 nm line for a range of 100–1100 cm⁻¹. Scanning electron microscopy (SEM) was carried out on a JEOL JSM-6390LV electron microscope. For these measurements, it was necessary to deposit a thin film of gold on the samples to improve their conductivity. Electrochemical measurements were performed using a three-electrode electrochemical cell as reported previously.^{30,31} The measurements were carried out in 1 M LiClO₄/propylene carbonate solution, which acted as the electrolyte, using a scan rate of 10 mV s⁻¹ through the voltage range of -0.5 V to 0.25 V. This range was limited by the need to have no remnant Li charge inside the V₂O₅ host at the end of each intercalation/deintercalation cycle i.e. the need to always have a closed loop in the voltammograms. The area of the working electrode exposed to the electrolyte was 1 cm².

Results and Discussion

The as-deposited coatings are stable in air for over 6 months presenting similar structural, morphological and electrochemical characteristics. In addition, the yellowish oxide coverage is uniform over the part of the substrate surface exposed to the electrolyte during electrodeposition. Figure 1 shows the XRD patterns of the oxide coatings

^zE-mail: dimitra@iesl.forth.gr

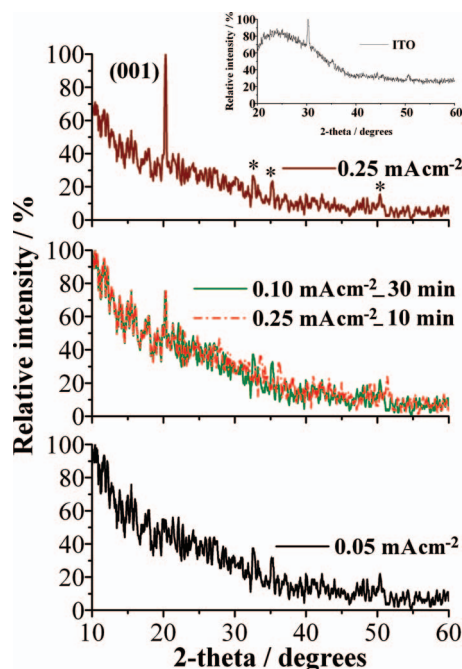


Figure 1. XRD patterns of the electrodeposited vanadium oxide coatings using deposition current densities of 0.05 mA cm^{-2} , 0.10 mA cm^{-2} for 30 min and 0.25 mA cm^{-2} for 10 and 30 min.

grown on ITO glass using deposition current densities of 0.05 mA cm^{-2} , 0.10 mA cm^{-2} and 0.25 mA cm^{-2} for the longest deposition time of 30 min. For the sample grown using 0.25 mA cm^{-2} , one characteristic peak at $2\theta = 20.3$ degs is observed, consistent to the (001) plane index of V_2O_5 .³¹ Regarding the sample grown using 0.10 mA cm^{-2} , the same characteristic peak is present, but with lower intensity and broader than in the case of 0.25 mA cm^{-2} , while there is no peak observed for the one grown using 0.05 mA cm^{-2} . Regarding the coatings deposited using smaller periods of time (10 and 20 min) the peak at 20.3 is present, but with lower intensity only for the 0.25 mA cm^{-2} case. The overlap of the XRD spectra for the oxides grown using deposition current density of 0.10 mA cm^{-2} for 30 min and 0.25 mA cm^{-2} for 10 min (Figure 1), i.e. with similar charge exchanged between the electrodes, indicates similar degree of crystallinity and deposited mass. In other words, this charge is a direct measure of the outcome of the electrochemical reaction taking place at the electrode as it would be expected from a faradaic process.

Raman spectra of the as-deposited samples grown after 30 min are shown in Figure 2. The peak positions agree with the V_2O_5 lines reported in the literature to within $\pm 2 \text{ cm}^{-1}$. The high-frequency peak at 995 cm^{-1} corresponds to the terminal oxygen ($\text{V}=\text{O}$) stretching mode, which results from unshared oxygen.³² Peaks at 705 and

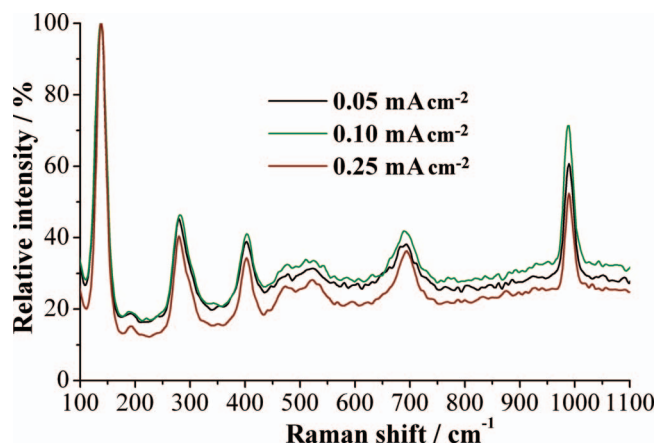


Figure 2. Raman spectra of the electrodeposited vanadium oxide coatings at room temperature using deposition current densities of 0.05 mA cm^{-2} , 0.10 mA cm^{-2} and 0.25 mA cm^{-2} for 30 min.

530 cm^{-1} can be attributed to stretching modes of the V-O-V bridging bonds with the bending motions of these bonds assigned to 484 and 304 cm^{-1} .^{33,34} The peaks at 405 and 283 cm^{-1} are assigned to the bending vibration of $\text{V}=\text{O}$ bonds.³³ Finally, two more low frequency Raman peaks at 195 and 143 cm^{-1} can be distinguished, which correspond to the lattice vibrations.^{34,35} However, it is observed that the peaks are more pronounced for the 0.25 mA cm^{-2} case, in accordance to the results of XRD analysis.

SEM images of the coatings grown using 0.05 mA cm^{-2} (a), 0.10 mA cm^{-2} (b) and 0.25 mA cm^{-2} (c) for 30 min are shown in Figure 3. The films mainly consist of elongated particles with sizes in the micron to submicron scales, joint together in random directions to form a rather rough, irregular surface. Increase of the deposition current density has the expected effect on the deposited mass as observed by comparing the coverage at the two lowest currents with no significant change in the size of the microcrystallites. Similar observations were made with the increase of deposition time. All combine to an apparent increase with current and time of the oxide's active volume i.e. the one accessible to charge through the porous morphology. It is thus expected that the electrochemical properties of 0.25 mA cm^{-2} – 30 min sample will be the best in the series.

Lithium charge intercalation/deintercalation of the vanadium oxide coatings as a function of current density is investigated by cyclic voltammetry. Figure 4a shows the voltammograms of the samples grown using 0.05 , 0.10 and 0.25 mA cm^{-2} for 30 min. Since, the value of the current density is a measure of the electrochemical activity of the electrode³⁶ it becomes evident that the material grown using 0.25 mA cm^{-2} surpasses all others by a considerable extent. Lithium charge intercalation/deintercalation of the vanadium oxide coatings as a function of current density is investigated by cyclic

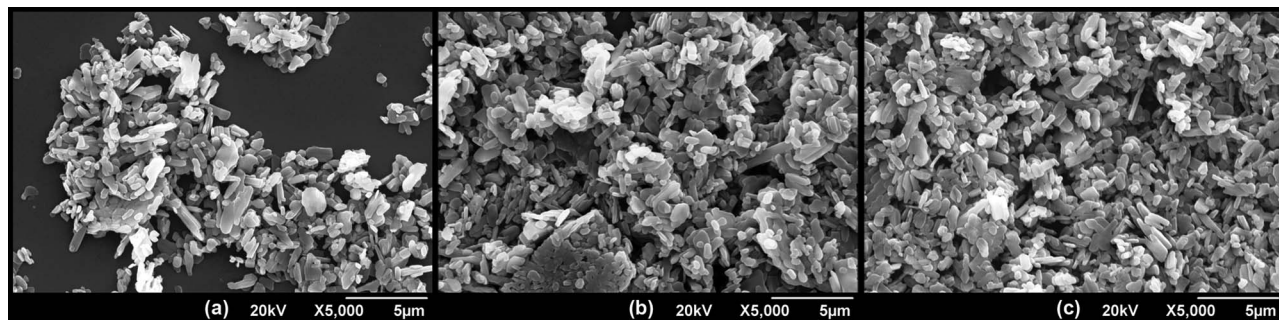


Figure 3. SEM images of as-deposited vanadium oxide samples using deposition current densities of (a) 0.05 mA cm^{-2} , (b) 0.10 mA cm^{-2} and (c) 0.25 mA cm^{-2} for 30 min.

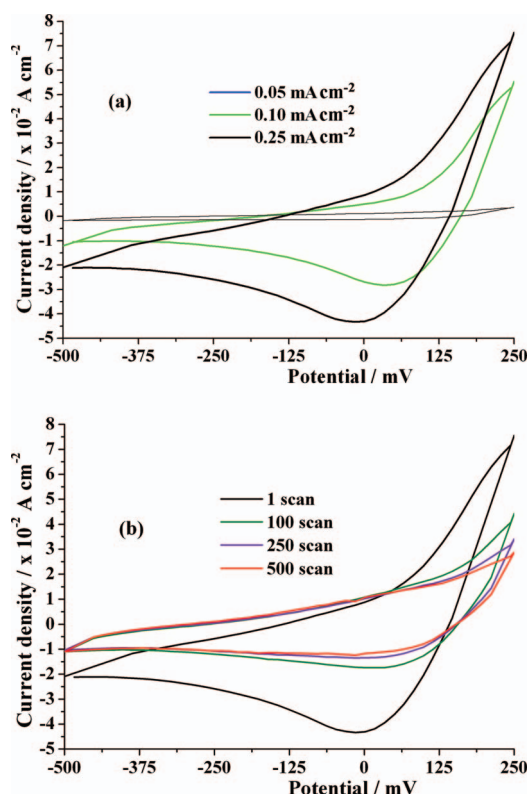


Figure 4. (a) Cyclic voltammograms for the vanadium oxide samples grown using deposition current densities of 0.05 mA cm^{-2} , 0.10 mA cm^{-2} and 0.25 mA cm^{-2} for 30 min and a scan rate of 10 mV s^{-1} . (b) Cyclic voltammograms for the as-deposited vanadium oxides using 0.25 mA cm^{-2} for scan numbers of 1, 100, 250 and 500.

voltammetry. Figure 4a shows the voltammograms of the samples grown using 0.05, 0.10 and 0.25 mA cm^{-2} for 30 min. Since, the value of the current density is a measure of the electrochemical activity of the electrode³⁶ it becomes evident that the material grown using 0.25 mA cm^{-2} surpasses all others by a considerable extent. The sta-

bility of this coating was studied by repeating the charging/discharging scan for 1, 100, 250 and 500 scans. Figure 4b shows that the charge current density decreases between the 1st and 100th scan, remaining almost constant afterwards. This behavior suggests a metastable initial material phase that stabilizes after the first few successive scans showing no further degradation in the time scales of our experiments. The maximum repeatable attained current density of $\sim 40 \text{ mA cm}^{-2}$ is comparable to V_2O_5 grown by electrodeposition (20 mA cm^{-2} ²⁷ and 60 mA cm^{-2} ²⁵) and better than V_2O_5 prepared by spin-coating (0.2 mA cm^{-2}),³⁷ sputtering (4 mA cm^{-2}),³⁸ sol-gel (2 mA cm^{-2}),³⁹ electrophoretic deposition ($20 \mu\text{A cm}^{-2}$)⁴⁰ and pulsed laser deposition (0.8 mA cm^{-2})⁴¹. Finally, all curves in Figure 4a display typical amorphous behavior since sharp peaks do not appear for either intercalation or deintercalation.^{42,43}

The switching response of the coating grown using 0.25 mA cm^{-2} for 30 min is studied by chronoamperometry (Figure 5a). Based on this curve, current vs. time log-log plots of all the temporal segments corresponding to intercalation and deintercalation processes are obtained. The intercalation process (Figure 5b) is found to decay in time as $t^{-1/2}$, which is associated with a proton diffusion-limited process. Regarding the deintercalation process (Figure 5c), the current follows a $t^{-3/4}$ dependence upon time, which is attributed to a control by a space charge limited lithium ion extraction mechanism. The dependence upon time for both processes is in agreement with previous reports.^{44,45}

The specific capacitance (in F/g) of the best sample is calculated according to the following equation¹⁶

$$C = \frac{Q}{\Delta V m}$$

where Q (in C) is the average charge interchanged between the electrode and the electrolyte during the charging and discharging process, m (in g) is the mass of the oxide and ΔV (in V) is the potential window. The mass of the deposited material (0.8 mg) is deduced by weighing the electrode before and after the coating, while the potential window is taken to be -0.5 V to $+0.25 \text{ V}$. Q is calculated by averaging the integrals of excess current density versus time curves of Figure 5a. We found that intercalated and deintercalated charge densities are similar to each other within 10% per cycle and equal to $87 \pm 9 \text{ mC cm}^{-2}$. This is a notable value considering earlier reports with sputtered ($24\text{--}27 \text{ mC cm}^{-2}$)⁴⁶ and sol-gel grown V_2O_5 (38 mC cm^{-2})⁴⁷. We attribute it to the increased coverage of the electrodeposited porous sample, which increases the surface exposed to the electrolyte giving Li cations access to a larger volume of the material. The specific capacitance of the

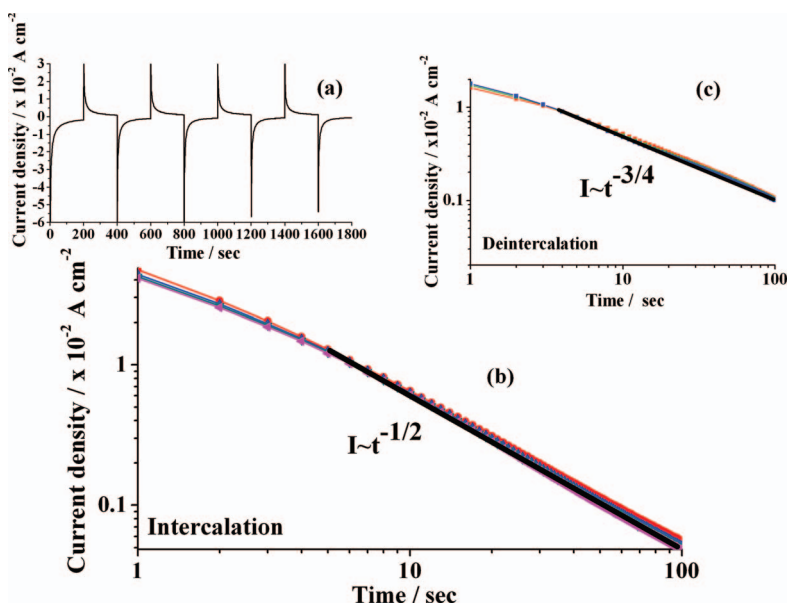


Figure 5. (a) The chronoamperometric response recorded at -0.5 V and $+0.25 \text{ V}$ at an interval of 200 s for the vanadium oxide samples grown using deposition current density of 0.25 mA cm^{-2} for 30 min. Logarithmic plots of the chronoamperometric response of vanadium oxide samples grown using deposition current density of 0.25 mA cm^{-2} corresponding to (b) intercalation and (c) deintercalation processes.

oxide is estimated to be 145 F g^{-1} . As the behavior of vanadium oxide coatings in $\text{LiClO}_4/\text{propylene carbonate}$ was not studied before, it is interesting to note that this film yields a capacitance of similar value with vanadium oxide in 2 M NaCl (114 F g^{-1}), in 2 M LiCl (122 F g^{-1})⁴ and in 3 M KCl (167 F g^{-1}).²⁵

Conclusions

Electrodeposition was employed to prepare vanadium oxide coatings at room temperature varying the deposition current density and time. The material was verified as V_2O_5 with a dense porous structure that revealed a crystalline signature albeit being prepared at ambient conditions. The coating grown at the upper extremum of parameter values showed the best electrochemical activity in terms of both interchanged charge and of specific capacitance. This notable response was attributed to the large exposed surface area that facilitates charge transfer between the oxide and the electrolyte.

References

1. A. Nishino, *J. Power Sources*, **60**, 137 (1996).
2. E. Faggioli, P. Rena, V. Danel, X. Andriu, R. Mallant, and H. Kahlen, *J. Power Sources*, **84**, 261 (1999).
3. A. Burke, *J. Power Sources*, **91**, 37 (2000).
4. R. N. Reddy and R. G. Reddy, *J. Power Sources*, **156**, 700 (2006).
5. B. E. Conway, *Electrochemical Supercapacitors*, Kluwer-Plenum Pub., New York, 1999.
6. E. Frackowiak and F. Béguin, *Carbon*, **39**, 937 (2001).
7. J. Chmiola, G. Yushin, Y. Gogotsi, C. Portet, P. Simon, and P. L. Taberna, *Science*, **313**, 1760 (2006).
8. M. Wu, G. A. Snook, G. Z. Chen, and D. J. Fray, *Electrochem. Commun.*, **6**, 499 (2004).
9. C. C. Hu, K. H. Chang, M. C. Lin, and Y. T. Wu, *NanoLett.*, **6**, 2690 (2006).
10. S. C. Pang, M. A. Anderson, and T. W. Chapman, *J. Electrochem. Soc.*, **147**, 444 (2000).
11. Q. T. Qu, Y. Shi, L. L. Li, W. L. Guo, Y. P. Wu, H. P. Zhang, S. Y. Guan, and R. Holze, *Electrochem. Commun.*, **11**, 1325 (2009).
12. X. P. Zhou, H. Y. Chen, D. Shu, C. He, and J. M. Nan, *J. Phys. Chem. Solids*, **70**, 495 (2009).
13. E. A. Ponzio, T. M. Benedetti, and R. M. Torresi, *Electrochim. Acta*, **52**, 4419 (2007).
14. Y. Wang and G. Z. Cao, *Adv. Mater.*, **20**, 2251 (2008).
15. Y. Wang, K. Takahashi, K. Lee, and G. Z. Cao, *Adv. Funct. Mater.*, **16**, 1133 (2006).
16. J. Yan, E. Khoo, A. Sumboja, and P. See Lee, *Nano*, **4**, 4247 (2010).
17. D. Vernardou, E. Spanakis, G. Kenanakis, E. Koudoumas, and N. Katsarakis, *Mater. Chem. Phys.*, **124**, 319 (2010).
18. J. Livage, *Chem. Mater.*, **3**, 578 (1991).
19. D. Vernardou, M. E. Pemble, and D. W. Sheel, *Chem. Vapor Depos.*, **13**, 158 (2007).
20. D. Vernardou, M. E. Pemble, and D. W. Sheel, *Chem. Vapor Depos.*, **12**, 263 (2006).
21. D. Vernardou, M. E. Pemble, and D. W. Sheel, *Surf. Coat. Tech.*, **188–189**, 250 (2004).
22. T. D. Manning, I. P. Parkin, M. E. Pemble, D. Sheel, and D. Vernardou, *Chem. Mater.*, **16**, 744 (2004).
23. T. D. Manning, I. P. Parkin, R. J. H. Clark, D. Sheel, M. E. Pemble, and D. Vernardou, *J. Mater. Chem.*, **12**, 2936 (2002).
24. J. W. Lee and S. I. Pyun, *J. Power Sources*, **119–121**, 760 (2003).
25. C. C. Hu, C. M. Huang, and K. H. Chang, *J. Power Sources*, **185**, 1594 (2008).
26. J. K. Lee, G. P. Kim, I. Kyu Song, and S. H. Baeck, *Electrochem. Commun.*, **11**, 1571 (2009).
27. J.-M. Li, K.-H. Chang, and C.-C. Hu, *Electrochem. Commun.*, **12**, 1800 (2010).
28. A. Ghosh, E. J. Ra, M. Jin, H.-K. Jeong, T. H. Kim, C. Biswas, and Y. H. Lee, *Adv. Funct. Mater.*, **21**, 2541 (2011).
29. C.-M. Huang, C.-C. Hu, K.-H. Chang, J.-M. Li, and Y.-F. Li, *J. Electrochem. Soc.*, **156**, A667 (2009).
30. D. Vernardou, H. Drosos, E. Spanakis, E. Koudoumas, C. Savvakis, and N. Katsarakis, *J. Mater. Chem.*, **21**, 513 (2011).
31. D. Vernardou, P. Paterakis, H. Drosos, E. Spanakis, I. M. Povey, M. E. Pemble, E. Koudoumas, and N. Katsarakis, *Sol. Energ. Mat. Sol. C*, **95**, 2842 (2011).
32. R. J. H. Clark, *The Chemistry of Titanium and Vanadium*, Elsevier, New York, 1968.
33. C. Julien, G. A. Nazri, and O. Bergstrom, *Phys. Stat. Sol.*, **201**, 319 (1997).
34. L. Abello, E. Husson, Y. Repelin, and G. Lucazeau, *Spectrochim. Acta Part A*, **39**, 641 (1983).
35. J. M. Jehng, F. D. Hardcastle, and I. E. Wachs, *Solid State Ionics*, **32/33**, 904 (1983).
36. J. P. Cronin, S. R. Kennedy, A. Agrawal, T. J. Gudgel, Y. J. Yao, J. C. L. Tonazzi, and D. R. Uhlmann, *Ceram. Trans.*, **92**, 175 (1999).
37. M. B. Sahana, C. Sudakar, C. Thapa, G. Lawes, V. M. Naik, R. J. Baird, G. W. Auner, R. Naik, and K. R. Padmanabhan, *Mater. Sci. Eng. B*, **143**, 42 (2007).
38. M. Benmoussa, A. Outzourhit, A. Bennouna, and E. L. Ameziane, *Thin Solid Films*, **405**, 11 (2002).
39. J. Livage, *Solid State Ionics*, **86–88**, 935 (1996).
40. W. G. Menezes, D. M. Reis, T. M. Benedetti, M. M. Oliveira, J. F. Soares, R. M. Torresi, and A. J. G. Zarbin, *J. Colloid Interf. Sci.*, **337**, 586 (2009).
41. G. J. Fang, Z. L. Liu, Y. Wang, Y. H. Liu, and K. L. Yao, *J. Vac. Sci. Technol. A*, **19**, 887 (2001).
42. L. H. M. Krings and W. Talen, *Sol. Energ. Mat. Sol. C*, **54**, 27 (1998).
43. K. Muthu Karuppasamy and A. Subrahmanyam, *Sol. Energ. Mater. Sol. C*, **92**, 1322 (2008).
44. C. G. Granqvist, *Handbook of Inorganic Electrochromic Materials*, Elsevier, Amsterdam, 1995.
45. B. W. Faughnan, R. S. Crandall, and M. H. Lampert, *Appl. Phys. Lett.*, **27**, 275 (1975).
46. D. Wruck, S. Ramamurthi, and M. Rubin, *Thin Solid Films*, **182**, 79 (1989).
47. N. Özer, *Thin Solid Films*, **305**, 80 (1997).